Z. Phys. D – Atoms, Molecules and Clusters 18, 287–298 (1991)

Atoms, Molecules and Clusters
Zeitschrift für Physik D

Diabatic representation for the excited states of the Na_2 molecule: application to the associative ionization reaction between two excited sodium atoms

A. Henriet, F. Masnou-Seeuws, and O. Dulieu

Laboratoire des Collisions Atomiques et Moléculaires (URA 281 du CNRS) Bât. 351, Université Paris-Sud, F-91405 Orsay Cedex, France

Received 20 September 1990; final version 20 November 1990

Abstract. A two-electron model potential method is proposed to compute diabatic electronic excited states for Na_2. The configuration space is first divided into two subspaces corresponding to singly and doubly excited configurations respectively. Next this partition is modified to ensure a correct dissociation limit for the ground state. The matrix element of the electronic Hamiltonian between the two subspaces can be extrapolated along a Rydberg series up to the ionization continuum. The first order M.Q.D.T. treatment of Giusti (1980) is then used to estimate the cross-sections for the reaction $Na(3p)+Na(3p) \rightarrow Na_2^+ + e^-$, considering various symmetries of the intermediate Na_2 molecule. A marked selectivity in favour of the $^3\Sigma_u^+$ symmetry is found and the estimated cross-section $\sigma \approx 5$ Å^2 for a collision energy of 0.05 eV is in satisfactory agreement with the experimental results.

PACS: 34.20b; 31.50+w; 34.50

1. Introduction

Being a simple example for the formation of a chemical bond, the associative ionization reaction:

$$Na(3p)+Na(3p) \rightarrow Na_2^+ + e^-, \quad (1)$$

has been the subject of much experimental investigation [1–6]. The most striking result at thermal energies is the marked dependence of the cross-section upon the preparation of the colliding atoms in particular magnetic sublevels $|Jm\rangle$. As discussed in several papers [7, 8], this anisotropy should be qualitatively explained by a strong selectivity of the molecular autoionization process:

$$Na_2^{**}(^{2S+1}\Lambda) \rightarrow Na_2^+ + e^-, \quad (2)$$

with respect to the symmetry of the electronic molecular state involved in the reaction (2). It is then, of course, necessary to assume that a given preparation of the colliding atoms [9] may lead to a selective population of one molecular symmetry:

$$Na(3p\,Jm)+Na(3p\,Jm) \rightarrow Na_2^{**}(^{2S+1}\Lambda) \quad (3)$$

The treatment of the autoionization process requires a knowledge of the potential curves and dynamical couplings for the Na_2 molecule. Adiabatic calculations have been performed, in the framework of a two-electron pseudo-potential [10, 11] or model potential [12, 13] approach, for the Σ, Π and Δ electronic excited states up to the $3p+3p$ dissociation limit. The comparison between the experimental and the theoretical spectroscopic constants [13] provides a check of the accuracy of the calculations, which is estimated around 1%. Moreover, adiabatic molecular quantum defects can be deduced from the calculations [12] and compared with the results of a fit to experimental data [14].

However, the adiabatic picture is not well adapted to the treatment of the dynamical problem: it is more convenient to develop a diabatic picture so as to treat the molecular autoionization in the framework of the Multichannel Quantum Defect Theory (MQDT) first developed by Giusti [15] for the inverse process (dissociative recombination) and next applied to the H+H associative ionization [16].

In the diabatic treatment, the electronic Hamiltonian is diagonalized separately within two subspaces [17], corresponding to singly and to doubly excited states respectively. The Na_2 Rydberg molecule is considered as a two-electron system, with a Rydberg electron bound to the Na_2^+ core which *is either in the ground state or in an excited state.* For a given symmetry, one then considers simultaneously singly-excited Rydberg series converging to the ground state of Na_2^+, and doubly-excited states.

The physical quantities involved in the MQDT treatment are, for each internuclear distance R, the quantum defect $\mu^l(R)$ associated with a Rydberg series, the potential energies $E_i(R)$ of the various doubly excited states,

and an "energy-normalized" form [8] $\mathscr{V}_i^l(R)$ of the electronic coupling between the two subspaces. The quantities $\mu_l(R)$ and $\mathscr{V}_i^l(R)$ should be nearly constant along the series l, in agreement with the typical behaviour of unperturbed Rydberg series [18]. It is then possible to extrapolate such quantities from low Rydberg states where accurate calculations are available up to the ionization continuum, so that the method avoids an explicit calculation of the final electronic state $Na_2^+ + e^-$.

Obviously, this picture of a Rydberg molecule is no longer valid at large internuclear distances, where the Na_2^+ core is parting into two cores.

The aim of the present paper is to report for model potential calculations concerning the diabatic excited states of Σ, Π and Δ symmetry in the Na_2 molecule. We shall check the validity of the Rydberg molecule picture by evaluating the parameters $\mu^l(R)$ and $\mathscr{V}_i^l(R)$ for various states of a given series. We shall also provide an estimation for the cross-sections of the associative ionization reaction using a first order MQDT treatment for the direct molecular autoionization process. A more refined treatment of the dynamical problem will be presented in a following paper.

Atomic units will be used, except otherwise stated.

2. Quasi-diabatic states

2.1. Principle of the method

As we have given in [13], hereafter referred to as paper *I*, a detailed presentation of the two-electron model potential method, we shall recall briefly the main lines of this treatment.

A two-electron model Hamiltonian:

$$\mathscr{H}(1,2) = h(1) + h(2) + \frac{1}{r_{12}} + V_{\text{diel}} \tag{4}$$

is considered, where $h(i)$ is the one electron model potential describing the motion of the electron (i) in the field of the two Na^+ cores at a distance R, $1/r_{12}$ is the two-electron interaction and V_{diel} a cross-polarization term.

The two-electron Na_2 wave function is expanded as:

$$\Psi(1,2) = \sum_{ab} \beta_{ab}[\phi_a(1)\,\phi_b(2) \pm \phi_a(2)\,\phi_b(1)] \tag{5}$$

where the orbitals $\phi(i)$ are eigenfunctions of the Na_2^+ Hamiltonian.

In contrast with paper *I*, and in view of the physical interpretation given below, we have not used a screened Na_2^+ Hamiltonian, so that the present results correspond to adiabatic potential curves that are slightly less accurate.

The list of the configurations that we have considered is given in paper *I* and in [19]. We have also described in there the numerical method used to compute the matrix elements of $\mathscr{H}$ (1, 2).

In order to enlighten the following discussion, the energies of the Na_2^+ orbitals are represented in Fig. 1.

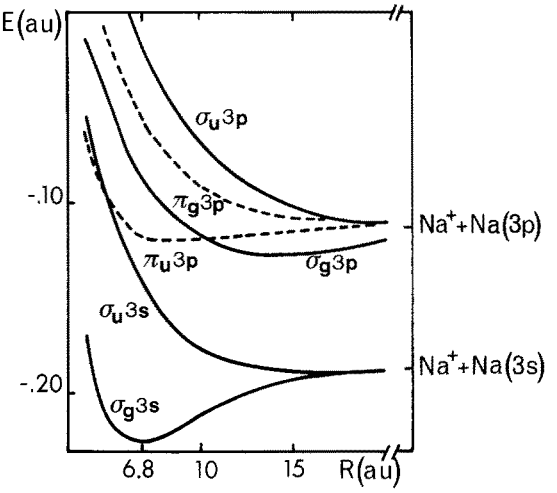

Fig. 1. Potential energy curves for the ground and first excited states of Na_2^+ (corresponding to the first orbitals used in the Na_2 treatment)

Next, instead of diagonalizing the hamiltonian in the full space of configurations, as in the adiabatic treatment, we define two subspaces P and Q, in which a partial diagonalization is performed. We have tried out several choices for the definition of the two subspaces. The calculations have been performed for a set of R values indicated in the following tables.

2.2. Diabatic "A" representation: quasi-diabatic states

A straightforward partition of the configuration space, in the spirit of the "quasi-diabatic" representation proposed by Sidis and Lefebvre-Brion [20] defines two subspaces [17] P^A and Q^A where:

i) P^A includes all the configurations containing the ground state orbital $\sigma_g 3s$ of the Na_2^+ molecular ion.

ii) Q^A includes all the other configurations. After diagonalization within the two subspaces Q^A and P^A, we obtain eigenstates $\mathscr{Q}_i^A$ and $\mathscr{P}_j^A$ such that:

$$\langle \mathscr{Q}_i^A | \mathscr{H}(1,2) | \mathscr{Q}_{i'}^A \rangle = F_i(R)\,\delta_{ii'} \tag{7}$$

$$\langle \mathscr{P}_j^A | \mathscr{H}(1,2) | \mathscr{P}_{j'}^A \rangle = E_j(R)\,\delta_{jj'} \tag{8a}$$

$$E_j(R) = \mathscr{E}_0(R) - \frac{1}{2(n_j^*(R))^2}\,\delta_{jj'} \tag{8b}$$

$$\langle \mathscr{P}_j^A | \mathscr{H}(1,2) | \mathscr{Q}_i^A \rangle = (n_j^*(R))^{-3/2}\,\mathscr{V}_{ij}(R) \tag{9}$$

The quantities F_i, E_j, n_j^*, $\mathscr{V}_{ij}$ for the two symmetries $^1\Sigma_g^+$ and $^3\Sigma_u^+$ are displayed in the Tables 1 and 2 for some values of the internuclear distance R. The diabatic potential curves $F_i(R)$ and $E_j(R)$ are drawn in the Figs. 2a and 3 together with the potential curve $\mathscr{E}_0(R)$ of the Na_2^+ ground state. It is clear that for $R < 10$ au, several Rydberg series, hereafter labelled "l", can be identified and associated with a quantum defect μ^l such that

$$n_j^*(R) \cong n^l - \mu^l(R) \quad n^l \geq l+1 \tag{10}$$

Table 1a. Energies $F_i(R)$ and $E_j(R)$, effective quantum numbers $n_j^*(R)$ and scaled electronic interactions (see Eqs. (7), (8), (9) in text) for the diabatic states of Na_2 of $^1\Sigma_g^+$ symmetry computed through the "A" procedure

$^1\Sigma_g^+$	Method A						
			Subspace P^A				
			"s" series			"d" series	
R(a.u.)		j	2	4	6	3	5
		E_j(a.u.)	−0.2724	−0.2429	−0.2301	−0.2657	−0.2400
		n_j^*	2.80	3.82	4.82	2.96	3.99
	Subspace Q^A						
5	i	F_i(a.u.)	Normalized electronic couplings $\mathcal{V}_{ij}(R)$				
	1	−0.2388	0.060	0.051	0.041	0.066	0.060
	2	−0.1947	0.016	0.009	0.010	0.053	0.057
	3	−0.1443	0.028	0.008	0.006	0.015	0.025
	P^A	E_j(a.u.)	−0.2862	−0.2568	−0.2440	−0.2795	−0.2543
	Q^A	n_j^*	2.81	3.84	4.86	2.97	3.99
6	i	F_i(a.u.)	Normalized electronic couplings $\mathcal{V}_{ij}(R)$				
	1	−0.2668	0.068	0.057	0.045	0.052	0.049
	2	−0.2082	0.018	0.060	0.010	0.030	0.038
	3	−0.1718	0.010	0.027	0.021	0.030	0.023
	P^A	E_j(a.u.)	−0.2836	−0.2546	−0.2421	−0.2758	−0.2518
	Q^A	n_j^*	2.84	3.89	4.94	3.04	4.06
8	i	F_i(a.u.)	Normalized electronic couplings $\mathcal{V}_{ij}(R)$				
	1	−0.2982	0.073	0.063	0.053	0.046	0.040
	2	−0.2205	0.019	0.001	0.004	0.026	0.029
	3	−0.2077	0.050	0.033	0.025	0.013	0.008
	P^A	E_j(a.u.)	−0.2706	−0.2429	−0.2308	−0.2621	−0.2401
	Q^A	n_j^*	2.89	3.94	4.99	3.11	4.13
10	i	F_i(a.u.)	Normalized electronic couplings $\mathcal{V}_{ij}(R)$				
	1	−0.3204	0.065	0.067	0.044	0.003	0.002
	2	−0.2320	–	–	–	–	–
	3	−0.2217	–	–	–	–	–

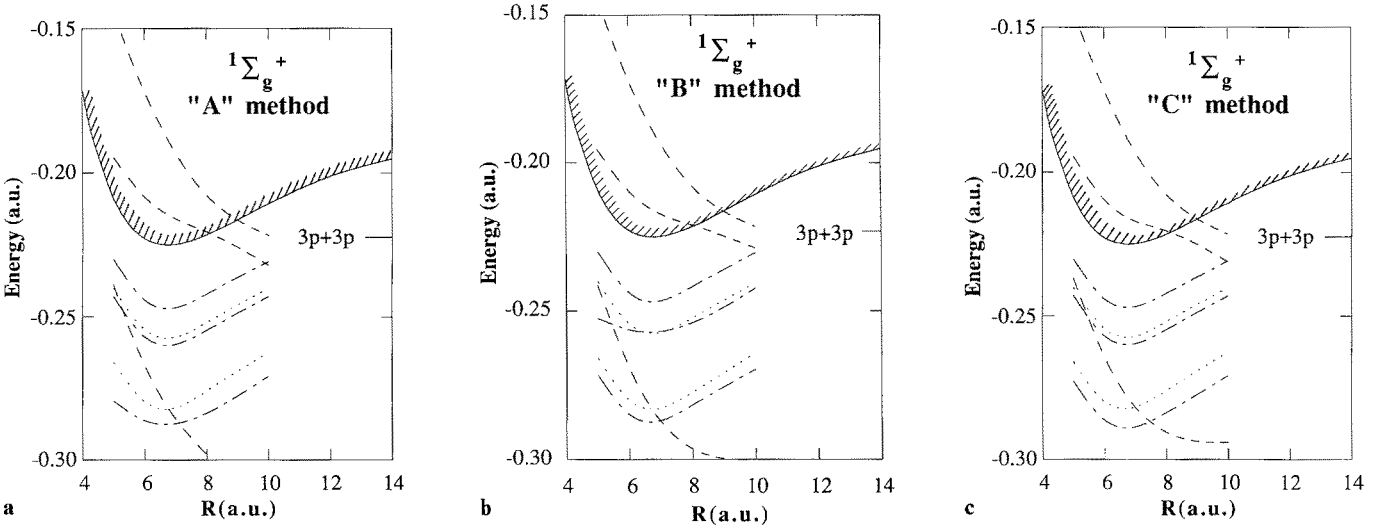

Fig. 2a–c. Diabatic potential curves of $^1\Sigma_g^+$ symmetry computed with three different methods (see text) **a** "A" procedure, **b** "B" procedure, **c** "C" procedure. Dash-dotted lines. "s" Rydberg curves $E_j(R)$, dotted lines: "d" Rydberg curves $E_j(R)$, broken lines: doubly excited curves $F_i(R)$

Table 1b. Same as Table 1a in case of the "B" procedure

$^1\Sigma_g^+$		Method B					
			Subspace P^B				
			"s" series			"d" series	
R (a.u.)		j	2	4	6	3	5
		E_j(a.u.)	−0.2715	−0.2524	−0.2300	−0.2657	−0.2400
		n_j*	2.82	3.84	4.83	2.96	3.99
5	Subspace Q^B i	F_i(a.u.)	Normalized electronic couplings $\mathcal{V}_{ij}(R)$				
	1	−0.2414	0.070	0.059	0.049	0.077	0.071
	2	−0.1953	0.017	0.008	0.057	0.053	0.057
	3	−0.1442	0.029	0.009	0.006	0.030	0.025
6	P^B / Q^B	E_j(a.u.)	−0.2848	−0.2562	−0.2439	−0.2799	−0.2542
		n_j*	2.84	3.87	4.87	2.96	3.99
	i	F_i(a.u.)	Normalized electronic couplings $\mathcal{V}_{ij}(R)$				
	1	−0.2691	0.077	0.061	0.046	0.062	0.059
	2	−0.2095	0.020	0.060	0.046	0.043	0.050
	3	−0.1718	0.010	0.020	0.015	0.030	0.026
8	P^B / Q^B	E_j(a.u.)	−0.2814	−0.2539	−0.2418	−0.2771	−0.2523
		n_j*	2.89	3.93	4.97	3.00	4.03
	i	F_i(a.u.)	Normalized electronic couplings $\mathcal{V}_{ij}(R)$				
	1	−0.2965	0.069	0.051	0.035	0.057	0.054
	2	−0.2210	0.025	0.033	0.047	0.010	0.010
	3	−0.2078	0.004	0.031	0.022	0.004	0.035
10	P^B / Q^B	E_j(a.u.)	−0.2694	−0.2423	−0.2303	−0.2638	−0.2404
		n_j*	2.92	3.98	5.05	3.07	4.09
	i	F_i(a.u.)	Normalized electronic couplings $\mathcal{V}_{ij}(R)$				
	1	−0.2999	0.066	0.067	0.059	0.003	0.002
	2	−0.2287	–	–	–	–	–
	3	−0.2214	–	–	–	–	–

In (10) n^l is the principal quantum number (varying from 3 to 5 or 6 in our present calculations) and $\mu^l(R)$ varies little from one value of j to the next one. We have already discussed in [12] the identification of the $^1\Sigma_g^+$ series as "s" and "d" series. The two quantum defects μ^s and μ^d vary only of a few percent when j is changed, the ground state being not considered here and the first excited state differing more markedly from the rest of the series. In the same way, two $^3\Sigma_u^+$ series can be identified as "p" and "f" series, the lowest state being even more different than in the preceeding case.

We should remark that the present notation "l" does not mean that the corresponding Rydberg electronic states are eigenstates of the electronic orbital angular momentum. The problem of the "$s-d$" or "$p-f$" mixing will not be discussed in the present paper [14].

For a given symmetry, a scaled interaction between a doubly-excited state i and a Rydberg series "l" can be defined from the relation:

$$\mathcal{V}_{ij}(R) \cong \mathcal{V}_i^l(R) \text{ for all } n^l \qquad (11)$$

This energy normalized electronic coupling is roughly constant (within 20%) for the third and fourth levels of the "s" $^1\Sigma_g^+$ series and varies even less ($\sim 10\%$) between the first two levels of the "d" series. In the $^3\Sigma_u^+$ case (Table 2), it is striking that the doubly-excited states are not interacting with the "p" Rydberg series, and only with the "f" series. The scaled interaction $\mathcal{V}_{ij}(R)$ then varies by less than 5%.

For larger internuclear distances ($R \geq 10$ au) the molecular quantum defect or the scaled interaction $\mathcal{V}_{ij}(R)$ are no longer constant when the principal quantum number varies, and therefore cannot be extrapolated along a Rydberg series to the continuum.

The main disadvantage of the "A" representation is that the ground state $X\,^1\Sigma_g^+$ is not well represented, the lowest state in P^A having an unphysical dissociation limit. As a consequence, the connection between the computed doubly-excited states and physical states at large internuclear distances is impossible.

Table 1c. Same as Table 1a in case of the "*C*" procedure

$^1\Sigma_g^+$			Method C				
			Subspace P^C				
			"s" series			"d" series	
R (a.u.)		j	2	4	6	3	5
		E_j(a.u.)	− 0.2724	− 0.2429	− 0.2301	− 0.2657	− 0.2400
		n_j*	2.80	3.82	4.82	2.96	3.99
	Subspace Q^C						
5	i	F_i(a.u.)	Normalized electronic couplings $\mathcal{V}_{ij}(R)$				
	1	− 0.2369	0.061	0.051	0.048	0.067	0.062
	2	− 0.1945	0.015	0.006	0.010	0.043	0.050
	3	− 0.1440	0.028	0.008	0.030	0.019	0.004
	P^C	E_j(a.u.)	− 0.2862	− 0.2568	− 0.2440	− 0.2795	− 0.2543
	Q^C	n_j*	2.81	3.84	4.86	2.97	3.99
6	i	F_i(a.u.)	Normalized electronic couplings $\mathcal{V}_{ij}(R)$				
	1	− 0.2640	0.071	0.060	0.051	0.051	0.048
	2	− 0.2097	0.014	0.060	0.010	0.042	0.041
	3	− 0.1718	0.020	0.020	0.020	0.028	0.015
	P^C	E_j(a.u.)	− 0.2836	− 0.2546	− 0.2421	− 0.2758	− 0.2519
	Q^C	n_j*	2.84	3.89	4.94	3.04	4.06
8	i	F_i(a.u.)	Normalized electronic couplings $\mathcal{V}_{ij}(R)$				
	1	− 0.2905	0.080	0.069	0.061	0.037	0.033
	2	− 0.2204	0.015	0.005	0.030	0.025	0.029
	3	− 0.2077	0.050	0.022	0.020	0.005	0.004
	P^C	E_j(a.u.)	− 0.2706	− 0.2429	− 0.2308	− 0.2621	− 0.2401
	Q^C	n_j*	2.89	3.94	4.99	3.11	4.13
10	i	F_i(a.u.)	Normalized electronic couplings $\mathcal{V}_{ij}(R)$				
	1	− 0.2941	0.082	0.073	0.067	0.029	0.023
	2	− 0.2310	0.030	0.025	0.022	0.034	0.037
	3	− 0.2215	0.020	0.027	0.030	0.051	0.038

2.3. Diabatic "*B*" representation

We have proposed in [12] an alternative construction for the $^1\Sigma_g^+$ diabatic states, in which we have first diagonalized the Hamiltonian in the subspace of the two configurations $(\sigma_g 3s)^2$ and $(\sigma_u 3s)^2$, hereby defining two eigenstates X_B and Y_B, X_B being the lower one. The subspaces P^B and Q^B are then deduced from P^A and Q^A by replacing the configurations $(\sigma_g 3s)^2$ and $(\sigma_u 3s)^2$ by X_B and Y_B respectively. The present calculations differ from those reported in [12] because the Q_B subspace contains a larger number of configurations. The results are displayed in Table 1b and in Fig. 2b. They do not differ significantly from the previous ones; the second excited state has a quantum defect closer to those of the two other "*s*" states; in contrast, the deviation of the scaled interaction $\mathcal{V}_{ij}(R)$ from its average value $\mathcal{V}_i^1(R)$ are larger than in the previous case.

However, this procedure is far from providing a satisfactory ground state, demonstrating that the doubly excited configurations containing the $\pi_u 3p$, $\sigma_g 3p$, $\pi_g 3p$ and $\sigma_u 3p$ orbitals do contribute markedly to the ground state.

2.4. Diabatic "*C*" representation

A third method consists in diagonalizing first the P^A subspace, in order to obtain correct unperturbed Rydberg series. Calling X_C the lowest eigenstate, we define the subspace P^C by excluding X_C from P^A, while:

$$Q^C = Q^A \cup X_C \tag{12}$$

The doubly-excited states are next constructed by diagonalization within the Q^C subspace.

This procedure provides a ground state that is satisfactory. The singly-excited $^1\Sigma_g^+$ Rydberg series, together with the doubly-excited states and the interactions are presented in Fig. 2c and in Table 1c. However, like in the "*B*" case, the deviation of the scaled interaction $\mathcal{V}_{ij}(R)$ from its average value $\mathcal{V}_i^1(R)$ is larger than what was found in the "*A*" procedure.

$^3\Sigma_u^+$			Method A				
			Subspace P^A				
			"p" series			"f" series	
R (a.u.)		j	1	3	5	2	4
		E_j(a.u.)	− 0.2597	− 0.2371	− 0.2272	− 0.2415	− 0.2294
		n_j*	3.11	4.19	5.19	3.90	4.90
	Subspace Q^A						
5	i	F_i(a.u.)	Normalized electronic couplings $\mathcal{V}_{ij}$(R)				
	1	− 0.2060	0.00	0.00	0.00	0.018	0.019
	2	− 0.1610	0.00	0.00	0.00	0.048	0.046
	3	− 0.1433	0.00	0.00	0.00	0.013	0.013
	P^A	E_j(a.u.)	− 0.2749	− 0.2516	− 0.2416	− 0.2561	− 0.2438
	Q^A	n_j*	3.10	4.17	5.17	3.88	4.89
6	i	F_i(a.u.)	Normalized electronic couplings $\mathcal{V}_{ij}$(R)				
	1	− 0.2449	0.00	0.00	0.00	0.020	0.021
	2	− 0.2007	0.00	0.00	0.00	0.044	0.042
	3	− 0.1846	0.00	0.00	0.00	0.008	0.009
	P^A	E_j(a.u.)	− 0.2753	− 0.2512	− 0.2405	− 0.2566	− 0.2434
	Q^A	n_j*	3.05	4.11	5.14	3.78	4.78
8	i	F_i(a.u.)	Normalized electronic couplings $\mathcal{V}_{ij}$(R)				
	1	− 0.2752	0.00	0.00	0.00	0.036	0.036
	2	− 0.2271	0.00	0.00	0.00	0.048	0.043
	3	− 0.2049	0.00	0.00	0.00	0.009	0.011
	P^A	E_j(a.u.)	− 0.2674	− 0.2408	− 0.2298	− 0.2487	− 0.2338
	Q^A	n_j*	2.97	4.08	5.12	3.63	4.66
10	i	F_i(a.u.)	Normalized electronic couplings $\mathcal{V}_{ij}$(R)				
	1	− 0.2820	0.034	0.014	0.008	0.048	0.042
	2	− 0.2375	0.017	0.021	0.019	0.049	0.037
	3	− 0.2207	0.035	0.024	0.021	0.009	0.007

Table 2. Same as Table 1a for the $^3\Sigma_u^+$ symmetry

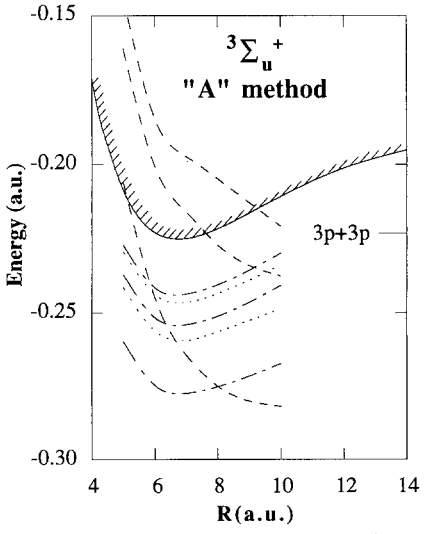

Fig. 3. Diabatic potential curves of $^3\Sigma_u^+$ symmetry computed in the framework of the "*A*" procedure (see text). Dash-dotted lines: "*p*" Rydberg curves $E_j(R)$, dotted lines: "*f*" Rydberg curves $E_j(R)$, broken lines: doubly excited curves $F_i(R)$

2.5. Discussion

We have also tried to define diabatic states in the framework of a procedure privileging the quality of the ground state $X\,^1\Sigma_g^+$. This state was computed with the best possible accuracy by diagonalization of the Hamiltonian within the full space of configurations. The subspace P was next constructed by orthogonalization of the mono-excited configurations to the X state, while Q was obtained by orthogonalization of the doubly-excited configurations to $X \cup P$. The resulting diabatic curves cannot be interpreted as unperturbed Rydberg series crossed by doubly-excited states, and therefore they are useless for our purpose. Details of the calculations are presented in [19].

The procedure "*C*" has been empirically found to be the best adapted one. However it appears from Fig. 2c and from Tables 1 that in the region of the minimum of the curve Na_2^+ ground state potential curve $\mathscr{E}_0(R)$ neither the diabatic curves nor the interactions differ markedly from the "*A*" to the "*C*" procedure.

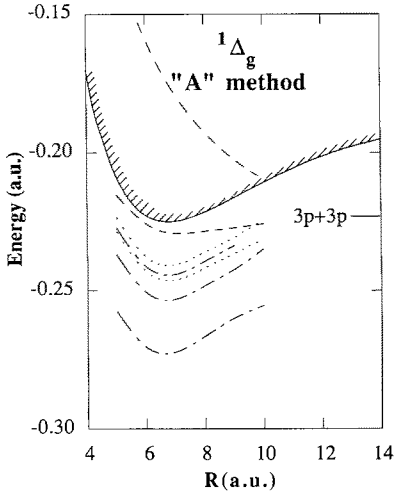

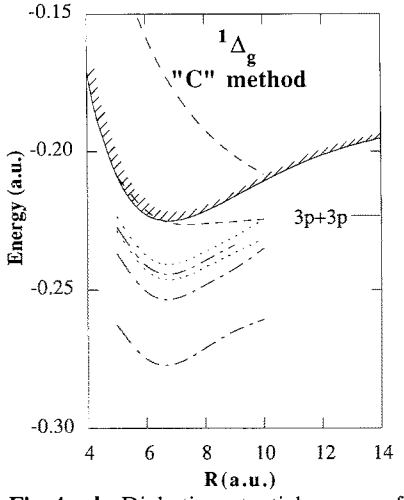

Fig. 4a, b. Diabatic potential curves of $^1\Delta_g$ symmetry computed with **a** "A" procedure, **b** "C" procedure. Dash-dotted lines: "d" Rydberg curves $E_j(R)$, dotted lines: "g" Rydberg curves $E_j(R)$, broken lines: doubly excited curves $F_i(R)$

Similar calculations have been performed for the other molecular symmetries. The $^3\Sigma_u^+$ diabatic states have been computed in the framework of the A method (see Table 2 and Fig. 3). The second and third doubly excited states are obviously correlated to the $3p+3p$ dissociation limit. One of the corresponding diabatic curves crosses the $\mathscr{E}_0(R)$ potential curve in the vicinity of the minimum.

For the other symmetries, we have compared the results of the "A" and of the "C" methods. They are generally little different except for the $^1\Delta_g$ symmetry (see Fig. 4a and 4b) where the first doubly-excited curve is shifted upward by diagonalization with the lowest state in P, which is more excited than in the $^1\Sigma_g^+$ case, its dissociation limit being Na(3s)+Na(3d) ($E=-0.2448$ au) instead of Na(3s)+Na(3s) ($E=-0.3777$ au). As a consequence, the first doubly-excited state, which is not crossing the curve $\mathscr{E}_0(R)$ in the "A" procedure, does cross it in the "C" procedure. The corresponding parameters are reported in Table 3. *The discussion on the associative ionization process is then influenced by the choice of the diabatization procedure.*

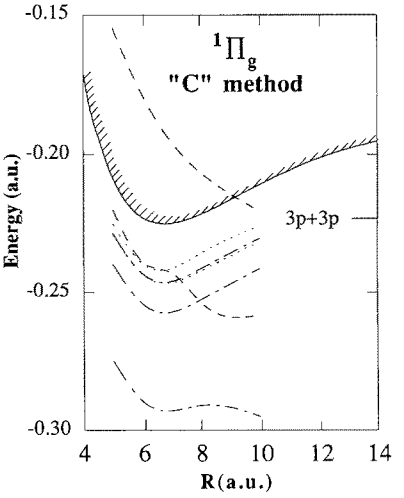

Fig. 5. Diabatic potential curves of $^1\Pi_g$ symmetry computed in the framework of the "C" procedure. Dash-dotted lines. "d" Rydberg curves $E_j(R)$, dotted lines: "g" Rydberg curves $E_j(R)$, broken lines: doubly excited curves $F_i(R)$

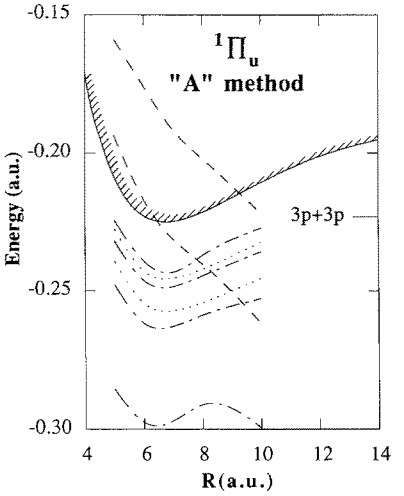

Fig. 6. Same as Fig. 5 for $^1\Pi_u$ symmetry computed in the framework of the "A" procedure. Dash-dotted lines: "p" Rydberg curves $E_j(R)$, dotted lines: "f" Rydberg curves $E_j(R)$, broken lines: doubly excited curves $F_i(R)$

The diabatic potential curves obtained in the framework of the "C" procedure are displayed in Figs. 5 to 9 for the $^1\Pi_g$, $^1\Pi_u$, $^3\Pi_g$, $^3\Pi_u$ and $^3\Delta_u$ symmetries. A summary of the parameters $\mu^l(R)$ and $\mathscr{V}_i^l(R)$ computed at the internuclear distance $R=6$ au is presented in Table 4 for all the molecular symmetries that can be populated starting from two Na(3p) atoms.

As will be discussed in Sect. 3, the key factor for the occurrence of the molecular autoionization process is the distance R_0 where a doubly-excited potential curve $F_i(R)$ is crossing the curve $\mathscr{E}_0(R)$. *It is obvious from the Figs. 2 to 9 that the existence and the location of such a crossing depend markedly upon the molecular symmetry that is considered, therefore indicating a strong selectivity of the molecular autoionization process.*

Table 3. Same as Table 1c for the $^1\Delta_g$ symmetry

$^1\Delta_g$		Method C					
			Subspace P^C				
			"d" series			"g" series	
R (a.u.)		j	1	2	4	3	5
		E_j(a.u.)	− 0.2628	− 0.2370	− 0.2273	− 0.2287	− 0.2235
		n_j*	3.04	4.19	5.17	4.99	5.80
5	Subspace Q^C i	F_i(a.u.)	Normalized electronic couplings $\mathcal{V}_{ij}(R)$				
	1	− 0.2087	0.00	0.081	0.083	0.00	0.003
	2	− 0.1297	0.00	0.00	0.00	0.00	0.00
	P^C	E_j(a.u.)	− 0.2751	− 0.2507	− 0.2413	− 0.2430	− 0.2377
	Q^C	n_j*	3.09	4.23	5.20	4.98	5.80
6	i	F_i(a.u.)	Normalized electronic couplings $\mathcal{V}_{ij}(R)$				
	1	− 0.2213	0.00	0.073	0.083	0.00	0.001
	2	− 0.1579	0.00	0.00	0.00	0.00	0.00
	P^C	E_j(a.u.)	− 0.2711	− 0.2482	− 0.2394	− 0.2418	− 0.2361
	Q^C	n_j*	3.18	4.33	5.29	4.97	5.86
8	i	F_i(a.u.)	Normalized electronic couplings $\mathcal{V}_{ij}(R)$				
	1	− 0.2260	0.00	0.056	0.056	0.002	0.002
	2	− 0.1920	0.00	0.00	0.00	0.00	0.00
	P^C	E_j(a.u.)	− 0.2649	− 0.2424	− 0.2338	− 0.2366	− 0.2307
	Q^C	n_j*	3.21	4.37	5.34	4.96	5.89
9	i	F_i(a.u.)	Normalized electronic couplings $\mathcal{V}_{ij}(R)$				
	1	− 0.2253	0.00	0.046	0.046	0.003	0.003
	2	− 0.2014	0.00	0.00	0.00	0.00	0.00

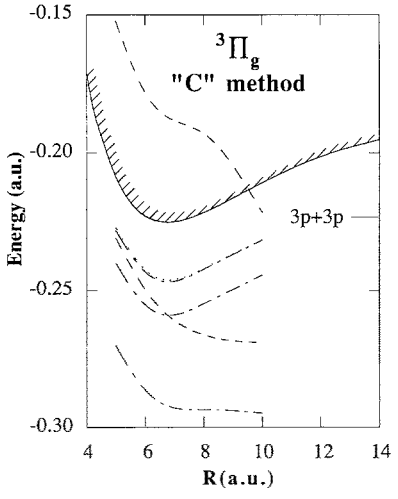

Fig. 7. Same as Fig. 5 for $^3\Pi_g$ symmetry. Dash-dotted lines: "d" Rydberg curves $E_j(R)$, dotted lines: "g" Rydberg curves $E_j(R)$, broken lines: doubly excited curves $F_i(R)$

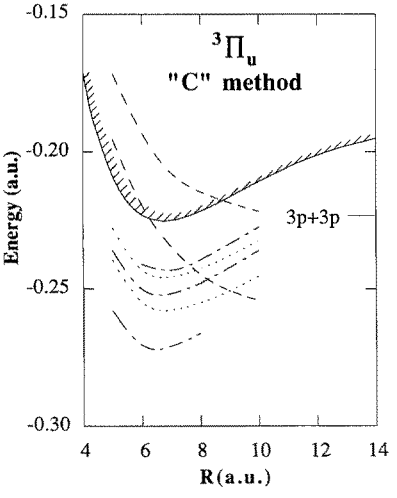

Fig. 8. Same as Fig. 5 for $^3\Pi_u$ symmetry. Dash-dotted lines: "p" Rydberg curves $E_j(R)$, dotted lines: "f" Rydberg curves $E_j(R)$, broken lines: doubly excited curves $F_i(R)$

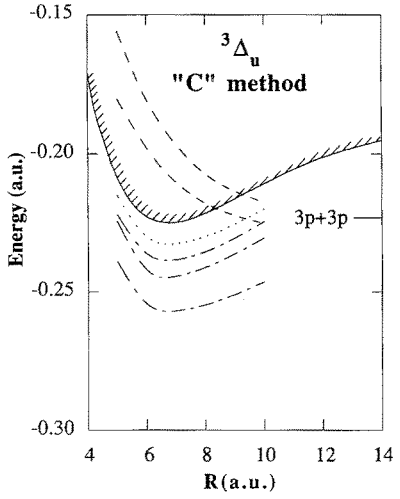

Fig. 9. Same as Fig. 5 for $^3\Delta_u$ symmetry. Dash-dotted lines: "f" Rydberg curves $E_j(R)$, dotted lines: "h" Rydberg curves $E_j(R)$, broken lines: doubly excited curves $F_i(R)$

Table 4. Average values for the parameters of the M.Q.D.T. treatment (see text) at an internuclear distance $R=6$ au

Symmetry	μ^l of the series	$\mathscr{V}_i^l(R)$		
		doubly excited state 1	doubly excited state 2	doubly excited state 3
$^1\Sigma_g^+$	"s": 0.15	0.06	0.04	0.02
	"d": 0.02	0.05	0.04	0.02
$^3\Sigma_u^+$	"p": 0.17	0.00	0.00	0.00
	"f": 0.12	0.02	0.04	0.00
$^1\Pi_g$	"d": 0.02	0.01	0.01	–
	"g": 0.05	0.01	0.01	–
$^3\Pi_g$	"d": 0.06	0.00	0.01	–
	"g": −0.05	0.00	0.00	–
$^1\Pi_u$	"p": −0.59	0.05	0.00	–
	"f": 0.01	0.02	0.02	–
$^3\Pi_u$	"p": −0.25	0.01	0.01	–
	"f": 0.03	0.03	0.02	–
$^1\Delta_g$	"d": −0.21	0.08	0.00	–
	"g": 0.11	0.00	0.00	–
$^3\Delta_u$	"f": −0.10	0.04	0.01	–

3. Application to the reaction $Na(3p)+Na(3p) \rightarrow Na_2^+ + e$

We shall first discuss how the molecular autoionization process (reaction 2) can be estimated from the present diabatic curves. Next, we shall present a simple model for the estimation of the cross-sections for the reaction (1).

3.1. Molecular autoionization: explanation of the selectivity

Assuming that a doubly excited molecular state $\mathscr{Q}_i^C$ is populated during a collision characterized by a center of mass energy E_T and a total angular momentum L, we consider the direct autoionization process:

$$Na_2^{**}(\mathscr{Q}_i^C, L) \rightarrow Na_2^+[X\,^2\Sigma_g^+, v, L] + e(\varepsilon, "l") \tag{13}$$

where the molecular ion Na_2^+ is formed in the ground electronic state, the vibrational and rotational states being v and L respectively. We assume that the total angular momentum $\hbar\sqrt{L(L+1)}$ of the heavy particle motion is conserved. An electron is ejected with energy ε in a continuum state which is the extrapolation of the singly-excited Rydberg series "l". Its wavefunction is asymptotically a Coulomb wavefunction with a phaseshift $\pi\mu^l$. *As discussed in Sect. 2.2, the notation "l" does not in general mean that the motion of the free electron is characterized by a unique partial wave.*

In the weak coupling approximation [15] the cross-section for the reaction (2) is given, at a collision energy E_T, by:

$$\sigma_{il}(E_T) = \frac{\pi}{2\mu E_T} r \sum_{L=0}^{L_{max}} (2L+1)\, a_{il}^L(E_T) \tag{14}$$

In (14), E_T is the collision energy, μ the reduced mass, r the multiplicity ratio between the final and the initial electronic state in (2) and $a_{il}^L(E_T)$ a dimensionless quantity such that:

$$a_{il}^L(E_T) = \sum_{v=0}^{v_{max}} \frac{4|\xi_{vL}^{il}|^2}{\left[1+\sum_{w=0}^{v_{max}} |\xi_{wL}^{il}|^2\right]^2}, \tag{15}$$

where the probability amplitude for the reaction (12) is estimated by:

$$\xi_{vL}^{il} = \pi \int \chi_{vL}(R)\, \mathscr{V}_i^l(R)\, \varphi_L^i(E_T, R)\, dR. \tag{16}$$

In (16) $\mathscr{V}_i^l(R)$ is the energy normalized coupling, defined by the equations (9) and (11), between the initial and final electronic state. $\chi_{vL}(R)$ is the vibrational wavefunction in the final state while $\varphi_L^i(E_T, R)$ is the energy-normalized radial wavefunction associated with the relative motion of the two atoms in the initial doubly-excited state.

The summation in (14) is over all the possible partial waves L in the reaction (13). It is controlled by considerations both on the initial and the final state of the nuclear motion. *The presence of a small barrier in the long range part of the potential $F_i(R)$ (see (7)) characteristic of the initial doubly electronic state can therefore significantly modify the value of L_{max} in (14).* In the present work, we have not considered such a possibility.

It appears (see for instance Tables 1–3) that the quantity $\mathscr{V}_i^l(R)$ is a slowly varying function of the internuclear distance R, so that

$$\xi_{vL}^{il} \cong \pi \bar{\mathscr{V}}_i^l \int \chi_{vL}(R)\, \varphi_L^i(E_T, R)\, dR \tag{17}$$

The molecular autoionization process is characterized both by the average value $\bar{\mathscr{V}}_i^l$ of the electronic coupling

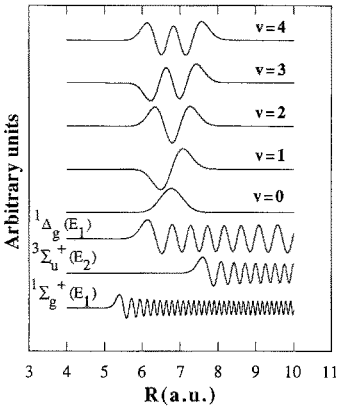

Fig. 10. Wavefunctions for the nuclear motion in the final and in the initial state as a function of the internuclear distance R. The three lower curves correspond to a collision with energy $E_T = 0.05$ eV, angular momentum $L=0$ and the potential of a doubly-excited state a) $^1\Sigma_g^+$ $F_1(R)$ b) $^3\Sigma_u^+$ $F_2(R)$ c) $^1\Delta_g$ $F_1(R)$. The five upper curves are the first vibrational wavefunctions for the Na_2^+ ground state

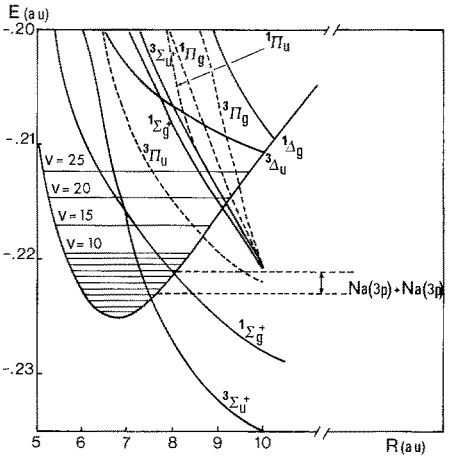

Fig. 11. Doubly-excited potential curves $F_2(R)$ (and $F_3(R)$ in the case of the $^1\Sigma_g^+$ and $^3\Sigma_u^+$ symmetries) correlated to the Na(3p) +Na(3p) dissociation limit. The full curves correspond to Σ and Δ states, the broken curves to Π states

Table 5. Values of the probability amplitude ξ_{vL}^{il} ($v=0$ and $v=4$) corresponding to a collision energy of 0.05 eV, an angular momentum $L=0$ and to the three potentials considered in Fig. 10 ($^1\Sigma_g^+$ $F_1(R)$, $^3\Sigma_u^+$ $F_2(R)$, $^1\Delta_g$ $F_1(R)$)

	$v=0$	$v=4$
$^3\Sigma_u^+$	0.139	1.150
$^1\Sigma_g^+$	10^{-6}	6.10^{-6}
$^1\Delta_g$	0.019	4.668

and by the Franck Condon factor for the initial and final nuclear wavefunctions. The strong selectivity as a function of the symmetry of the molecular doubly excited state $|i\rangle$ can therefore be qualitatively explained by considering the relative position of the curves $F_i(R)$ and $\mathscr{E}_0(R)$.

This is illustrated in Fig. 10 where we have represented both the first vibrational wavefunctions $\chi_{v0}(R)$ ($v=0$, 1, 2, 3, 4 and $L=0$) associated with the final state and the nuclear continuum radial wavefunctions $\varphi_0^1(E_T, R)$ or $\varphi_0^2(E_T, R)$, corresponding to a collision with energy 0.05 eV, angular momentum $L=0$, in the potential $F_1(R)$ (resp. $F_2(R)$) of the first doubly-excited state in the case of the $^1\Sigma_g^+$ and $^1\Delta_g$ symmetries and to the second doubly-excited state in the case of the $^3\Sigma_u^+$ symmetry*. It is obvious that the overlap is negligible in the first case and not in the two other ones. More quantitative conclusions can be drawn from Table 5, where typical values of the probability amplitude ξ_{vL}^{il} at a collision energy of 0.05 eV are presented.

*In the case of the $^1\Sigma_g^+$ symmetry, the lower doubly-excited curve $F_1(R)$ has been chosen as an example of a "non-crossing case". It will not be considered further in the discussion

3.2. *Calculations for the molecular autoionization process*

Starting from two separated atoms, the probability of populating a doubly-excited state $F_i(R)$ in a collision will depend upon the dynamics at large internuclear distances. One should consider, in the asymptotic region, adiabatic potential curves and dynamical couplings between them, in order to treat the collision problem for $R>10$ au. Then a frame transformation from the adiabatic to the present diabatic representation would provide a correct estimation of the various curves.

It is beyond the scope of the present paper to discuss the long range collision problem. Nevertheless, we shall qualitatively relate the computed diabatic curves to the separated atoms limit. In fact, besides the curves correlated to the Na(3p)+Na(3p) limit (with asymptotic energy $E_{cov}^{as} = -0.2230$), or to the neighbouring Na(3s)+Na(nl) limit one should consider ionic curves correlated to $Na^+ + Na^-$, Na^- being either in the ^1S ground state (the asymptotic energy being then $E_{ion}^{as} = -0.20896 - 1/R$), or in an excited state [22]. The ionic-covalent crossing is located at $R_C \cong 71$ au in the first case, but much closer for the other dissociation limits; for instance, the $Na^+ + Na^-$ ($3p^2\,^1D$) curve corresponds to an asymptotic energy $E_{ion}^{as} = -0.114 - 1/R$, so that the ionic covalent crossing is located at $R_C = 9.2$ au and could have to be considered in the present discussion.

From qualitative considerations, it is reasonable in most symmetries to assume that the second doubly-excited curve $F_2(R)$ curve is the most likely to be populated starting from two Na(3p) atoms. Indeed, after orthogonalization to the lowest state in the P subspace, the curve $F_1(R)$ should be correlated to an ionic dissociation limit. A look at Fig. 11 shows that for collision energies $E_c < 0.054$ eV, the molecular ionization process should proceed selectively via the curve $F_2(R)$ of $^3\Sigma_u^+$ symmetry. Using the method described in Sect. 3.1, and considering the scaled interaction with the "f" series presented in Table 2, we obtain from (14) a cross-section $\sigma_{2f}(E_T)$

$=(4/3)47$ Å^2 that is 62.7 Å^2 for $E_T=0.05$ eV. For such calculations, we have assumed that there is no long range barrier in the potential, so that the L_{max} value in (14) is determined only by the number of rotational levels corresponding to a given vibrational level of the curve $\mathscr{E}_0(R)$.

Assuming a statistical population sharing between the various molecular symmetries correlated to Na$(3p)$ + Na$(3p)$, the probability of populating one $^3\Sigma_u^+$ state is $\frac{3}{36}$, so that we end with a cross-section $\sigma \cong 5$ Å^2 for the reaction (1). This value is in reasonable agreement with the experimental value which is around 1–4 Å^2 [1–3, 23]. Moreover, out of the two curves $F_2(R)$ and $F_3(R)$, the lowest one is more likely to be populated from two $\sigma 3p$ orbitals, while the upper one contains a larger contribution of the $(\pi_g 3p)$ $(\pi_u 3p)$ configuration. *Therefore, the autoionization via the $^3\Sigma_u^+$ $F_2(R)$ doubly-excited diabatic curve could explain the experimental observation of the strong polarization dependence of the ion signal at collision energies around 0.05* eV.

However, especially in the case of potential curves of Δ symmetry (see Figs. 4 and 9) there is no obvious reason to disregard the possibility of populating the lowest doubly-excited curve $F_1(R)$. We have performed calculations for the autoionization process via the $^1\Delta_g(F_1)$ doubly excited curve, which is crossing the curve $\mathscr{E}_0(R)$ in the vicinity of the minimum. We find a cross-section $\sigma_{1d}(E_T)=19.2$ Å^2. Using again the very crude approximation of a statistical population sharing between 12 potential curves correlated to Na$(3p)$+Na$(3p)$, and assuming an adiabatic correlation from the $3p+3p$ limit to the curve $F_1(R)$, one obtains a cross-section for reaction (1) around 1 Å^2, also in agreement with the experimental results. Besides, our calculations show that the variation of the cross section as a function of the collision energy E_T is different in the case of molecular autoionization via a $^3\Sigma_u^+$ or via a $^1\Delta_g$ state [24]. The latest ionization channel being populated from two π atomic orbitals, this could lead to a modification of the polarization dependence of the cross-section when the collision energy is varied [23, 24].

In contrast, a look at Table 5 explains why, for *doubly-excited potential curves that are not crossing the ionic curve $\mathscr{E}_0(R)$ in the vicinity of the minimum, the computed autoionization cross-sections are several orders of magnitude smaller than the observed ones.*

3.3. Discussion

Both the limitations on the total number of configurations involved in the potential calculations, and the uncertainty on the choice of the diabatic procedure should lead us to consider an "error bar" in the parameters that we are using in the MQDT treatment. We have checked that the present first-order results are not significantly modified when one varies those parameters within the "error bar".

First, we have seen in Sect. 3 that the model of a Rydberg molecule is questionable for the internuclear distance $R=10$. In the case of molecular autoionization via the $^3\Sigma_u^+$ $F_2(R)$ potential curve, the scaled interaction $\mathscr{V}_2^f(R)$ deduced from the values of Table 2 has been modified to $\mathscr{V}_2'^f(R)$ by changing to 0 the value of $\mathscr{V}_2^f(R)$ for $R \geq 10$, and joining smoothly to the unmodified curve at $R \leq 8$. At a collision energy $E_T=0.05$ eV, the molecular autoionization cross-section σ_{2f} varies only from 63.7 Å^2 to 62.1 Å^2. Next we have modified $\mathscr{V}_2^f(R)$ to $\mathscr{V}_2^f(R)+\Delta V$, ΔV being a constant for all R values. The cross-section is modified from 63.7 Å^2 to 60.6 Å^2 for $\Delta V=+0.005$ and 66.9 Å^2 for $\Delta V=-0.005$. Finally, considering again the interaction $\mathscr{V}_2'^f(R)$ defined above, we have shifted the curve $F_2(R)$ by ΔE. The crossing point with $\mathscr{E}_0(R)$ is modified from 7.7 au to 7.5 au when $\Delta E=-0.002$ and to 7.8 au when $\Delta E=+0.002$. The cross section for reaction (3) is modified from $\sigma_{2f}=62.1$ Å^2 to 66.5 Å^2 and 54.8 Å^2. We therefore may conclude that the present accuracy of the $^3\Sigma_u^+$ diabatic potential curves is satisfactory for the present estimation of the cross-sections, bearing in mind the crude approximations on the population sharing.

Another check concerns the validity of the first-order approximation in the MQDT treatment. It has been performed and will be presented in a following paper [24]. The values for the total cross-section σ_{2f} at $E_T=0.05$ eV are not modified when second order effects are introduced. However, a different conclusion is obtained at lower energies.

The molecular autoionization process via the $^1\Delta_g$ $F_1(R)$ doubly-excited potential curves are more sensitive both to the accuracy of the computed potential curves and to the level of sophistication of the dynamical treatment.

4. Conclusion

We have computed diabatic curves at internuclear distances $R \leq 10$ au for the excited states of Na_2 by considering separately singly excited Rydberg series (one electron in the field of a ground state Na_2^+ core) and doubly excited states (one electron in the field of an excited state Na_2^+ core). We have deduced from these calculations molecular quantum defects for the Rydberg series and scaled interactions with the doubly-excited states. It is then possible to compute the cross-sections for the molecular autoionization of Na_2^{**} in the framework of the MQDT treatment proposed by Giusti [15]. It appears that this process should take place preferentially by population of the second doubly excited curve of $^3\Sigma_u^3$ symmetry; however, the first doubly excited curve of $^1\Delta_g$ symmetry could also be a good candidate especially at low collision energies provided it may be populated from two Na$(3p)$ atoms. The computed cross sections appear to be in satisfactory agreement with experiment.

This first order treatment will be improved in a following paper [24] by considering both:

i) second order terms in the computation of the direct autoionization process. Recent calculations have shown that the cross-sections at an energy E_T of 0.05 eV are not modified by the inclusion of those terms, while the

results at lower collision energies are significantly modified.

ii) the indirect autoionization process via an excited vibrational state of a singly-excited Rydberg electronic state:

$$Na_2^{**} \rightarrow Na_2^{*}(v', L) \rightarrow Na_2^{+}(v, L) + e^{-}$$

Indeed, the electronic coupling between a doubly-excited state and a Rydberg series *"l"* leads to a population transfer not only into the continuum electronic states but also to singly-excited Rydberg states. The vibrational ionization is then responsible, in a second step, for the ejection of the electron. The cross-section including both the direct and the indirect process will be presented in a forthcoming work [24]. A detailed comparison with the semi-classical calculations of Geltman [25] will be given therein.

Finally, future work should clarify the population of the various doubly-excited states starting from the separated atoms limit. The statistical population sharing assumed in the present work is certainly a crude approximation especially at low collision energies.

The authors are most grateful to Dr. Annick Giusti-Suzor for many helpful discussions and for making her computer code available.

References

1. Bezuglov, N.N., Klucharev, A.N., Sheverev, V.A.: J. Phys. B: At. Mol. Phys. **20**, 2497 (1987)
2. Huennekens, J., Gallagher, A.: Phys. Rev. A **28**, 1276 (1983)
3. Bonnano, R., Boulmer, J., Weiner, J.: Phys. Rev. A **28**, 604 (1983)
4. Kircz, J.G., Morgenstern, R., Nienhuis, G.: Phys. Rev. Lett. **48**, 610 (1982)
5. Meijer, H.A.J., Pelgrim, T.J.C., Heideman, H.G.M., Morgenstern, R., Andersen, N.: Phys. Rev. Lett. **59**, 2939 (1987) and references therein
6. Wang, M.X., Weiner, J.: Phys. Rev. A **42**, 675 (1990)
7. Jones, D.M., Dahler, J.S.: Phys. Rev. A **35**, 3688 (1987)
8. Weiner, J., Masnou-Seeuws, F., Giusti-Suzor, A.: Adv. At. Mol. Opt. Phys. **26**, 209 (1989)
9. Nienhuis, G.: Electronic and Atomic Collisions. p. 569. Invited papers of the XIV ICPEAC, Lorents, D.E., Meyerhof, W.E., Peterson, J.R. (eds.). New York: North Holland 1986
10. Jeung, G.H.: J. Phys. B: At. Mol. Phys. **16**, 4289 (1983)
11. Jeung, G.H.: Phys. Rev. A **35**, 26 (1987)
12. Henriet, A., Masnou-Seeuws, F.: J. Phys. B: At. Mol. Phys. **21**, L 339 (1988)
13. Henriet, A., Masnou-Seeuws, F.: J. Phys. B: At. Mol. Phys. **23**, 219 (1990)
14. Jungen, C., Masnou-Seeuws, F.: J. Phys. B: At. Mol. Phys. (to be published)
15. Giusti, A.: J. Phys. B: At. Mol. Phys. **13**, 3867 (1980)
16. Urbain, X.: (1990) Thesis Louvain La Neuve (unpublished)
17. O'Malley, T.: Adv. At. Mol. Phys. **7**, 223 (1971)
18. Bethe, H.A.: Intermediate quantum mechanics. p. 29. New York: Benjamin 1964
19. Henriet, A.: 1988 Thesis Orsay (Unpublished)
20. Sidis, V., Lefebvre-Brion, H.: J. Phys. B: At. Mol. Phys. **4**, 1040 (1971)
21. Norcross, D.W.: Phys. Rev. Lett. **32**, 192 (1974)
22. Dulieu, O.: Z. Phys. D-Atoms, Molecules and Clusters **13**, 17–24 (1989)
23. Meijer, H.A.J.: Z. Phys. D – Atoms, Molecules and Clusters **17**, 257 (1990)
24. Dulieu, O., Giusti-Suzor, A., Masnou-Seeuws, F.: J. Phys. B: At. Mol. Phys. (to be published)
25. Geltman, S.: J. Phys. B: At. Mol. Phys. **21**, L 735 (1988)